

Enhanced electronic polarizability of metallic stripes and the universality of the bond-stretching phonon anomaly in high-temperature cuprate superconductors

S. I. Mukhin,^{1,*} A. Mesaros,² J. Zaanen,² and F. V. Kusmartsev³

¹Theoretical Physics Department, Moscow Institute for Steel and Alloys, Moscow 119049, Russia

²Lorentz Institute for Theoretical Physics, Leiden University, Leiden NL-2333 CA, The Netherlands

³Department of Physics, Loughborough University, Loughborough, Leics LE11 3TA, United Kingdom

(Received 17 October 2007; published 28 November 2007)

We demonstrate that the strong anomalies in the high frequency LO-phonon spectrum in cuprate superconductors can, in principle, be explained by the enhanced electronic polarizability associated with the self-organized one dimensionality of metallic stripes. Contrary to the current interpretation in terms of transversal stripe fluctuations, the anomaly should occur at momenta parallel to the stripes. The doping dependences of the anomaly are naturally explained, and we predict that the phonon linewidth and the spread of the anomaly in the transverse momentum decrease with increasing temperature, while high resolution measurements should reveal a characteristic substructure to the anomaly.

DOI: [10.1103/PhysRevB.76.174521](https://doi.org/10.1103/PhysRevB.76.174521)

PACS number(s): 74.72.-h, 63.22.+m, 71.27.+a, 74.81.-g

I. INTRODUCTION

The phonon spectrum of the high- T_c superconducting cuprates is characterized by a peculiar anomaly: halfway the Brillouin zone, the bond-stretching Cu-O vibration mode seems to suddenly dip down to a much lower frequency.¹⁻³ The linewidth reaches its maximum at a wave vector somewhat shifted from the frequency-dip position, while it narrows at higher temperatures.⁴ In addition, the anomaly has a narrow intrinsic peak width as a function of momentum transversal to the mode propagation direction.⁴ While the position of the dip is doping independent, the softening amplitude changes with doping,^{3,5} tracking roughly the “Yamada plot.”⁶ This is hard to explain in a conventional fermiology framework, and interpretations invoking a coupling between the phonon and purely electronic collective modes of the stripes acquired credibility⁷ by the recent demonstration that the anomaly is particularly pronounced in $\text{La}_{2-1/8}\text{Ba}_{1/8}\text{CuO}_4$,^{3,4} a system with a well developed static stripe phase.⁸ Initially, Kaneshita *et al.*⁹ considered a crossing of the LO phonon with the transversal “meandering” stripe fluctuations¹⁰ by computing the Gaussian fluctuations around the Hartree-Fock stripe ground state. This interpretation is, however, problematic: it was deduced¹¹ using the anisotropy of the spin fluctuations that in the untwinned YBCO superconducting crystal, the phonon anomaly occurs for phonon wave vectors parallel to the stripes, at a right angle, as compared to the expectations for transversal stripe modes.

A well-known problem with the Hartree-Fock stripes is that they are “insulatinglike,”¹² while cuprate stripes are quite metallic. This supports the idea that they form an electronic liquid crystal of the smectic kind as introduced by Kivelson and co-workers.¹³ Here, the transversal modes are frozen out by commensuration effects, and instead, the low energy physics is governed by on-stripe compressional fluctuations. As one of us already noticed sometime ago,¹⁴ the electronic polarizability associated with the on-stripe Luttinger-liquid-like physics should be strongly enhanced at the on-stripe $2k_F$ wave vectors, and this feature might well

govern the phonon anomaly (see Fig. 1). This view is actually supported by numerous experimental and computational evidences. First of all, one-dimensional structure of the electron momentum distribution function is documented by angle resolved photoemission spectroscopy (ARPES) measurements in nonsuperconducting $\text{La}_{1.28}\text{Nd}_{0.6}\text{Sr}_{0.12}\text{CuO}_4$ in the commensurate static stripe phase at 1/8 hole doping.¹⁶ Besides, the high resolution ARPES data¹⁷ in high- T_c ($T_c = 40$ K) $\text{La}_{1.85}\text{Sr}_{0.15}\text{CuO}_4$, followed by a more detailed data for Sr concentration x ranging from $x=0.03$ to $x=0.3$,¹⁸ indicate a dual nature of the electronic spectrum, which contains one-dimensional straight segments in the momentum distribution of the spectral weight in the $(\pi, 0)$ and $(0, \pi)$ antinodal regions superimposed on the two-dimensional (2D)-like spectral weight distribution in the nodal direction $[1, 1]$ predicted by local-density approximation (LDA) calculations. These straight segments in the Brillouin zone would be expected to occur from one-dimensional (1D) stripes along the $[1, 0]$ and/or $[0, 1]$ direction in the CuO plane. The momentum distribution function integrated over 30 meV interval around the Fermi level, according in Ref. 17, suggests two sets of constant energy contours defined by the $|k_x| = \pi/4$ and $|k_y| = \pi/4$ lines, which would be, indeed, expected for superposition of two perpendicularly oriented stripe domains with quarter-filled charge stripes.¹⁶ The 1D-like spectral weight crosses the Fermi level at about the optimal doping $x=0.15$ in $\text{La}_{2-x}\text{Sr}_x\text{CuO}_4$.¹⁸ This same spectral weight is observed as a “flat band” or as the extended van Hove singularities below the Fermi level^{18,19} in the underdoped high- T_c cuprates, which are characterized with a transition into the pseudogap state. From the LDA+ U model computation¹⁵ side, there is also a prediction of metallic stripes with $4a_0$ (a_0 is the lattice constant in CuO plane) periodicity in $\text{La}_{15/8}\text{Sr}_{1/8}\text{CuO}_4$ high- T_c compound. The calculations give the semiflat pieces of the quasi-1D Fermi surface due to small interstripe hybridization $t_\perp \approx 15$ meV. Besides, recent scanning tunneling microscopy measurements²⁰ in the so-called electronic cluster glass state of strongly underdoped Na-CCOC and Dy-Bi2212 cuprates have revealed “nanostripe domains” with a short-range $4a_0$ interstripe

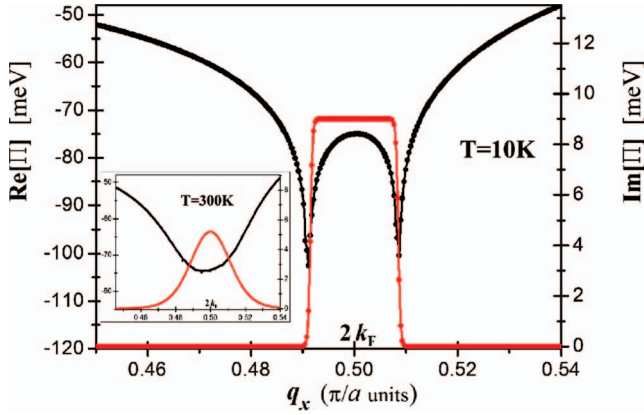


FIG. 1. (Color) Real (black line) and imaginary (red line) parts of the on-stripe electronic phonon self-energy $\Pi(q_x, \omega)$ at $T=10$ K at a fixed (phonon) frequency $\omega=68$ meV as a function of the momentum component q_x parallel to the stripes, taking for the dimensionless electron-phonon coupling a value representing the cuprates: $\xi=1.0$. In the inset, the results are shown at a higher $T=300$ K.

periodicity. In this relation, we mention that, as will become clear from the presented here derivations, the stripe-induced LO-phonon softening effect considered in our work is independent of the length of the stripe segments as long as the latter are longer than, e.g., 10–20 lattice constants in the CuO plane, such that quantum size gap in the electronic spectrum related with unidirectional motion along the finite length segment is substantially below the optical phonon frequency of ~ 0.1 eV.

Here, we analyze the phonon anomaly as associated with an array of Luttinger liquids embedded into a 2D optical phonon background. We employ two simplifying assumptions. (i) We use the free fermion charge susceptibility (Lindhardt function) instead of the fully interacting Luttinger liquid form, since the phonon anomaly appears to be in first instance sensitive only to the gross features of the 1D electron dynamics. (ii) More critical, we assume that at the energy of the anomaly, $\omega_{LO} \sim 68$ meV, the interstripe hopping $\propto t_{\perp}$, and interaction effects can be neglected. Our theory gives a number of straightforward *a posteriori* explanations of the experiment as well as provides several important predictions that are within reach of experiment. The list of both the explanations (three) and predictions (four), which follow from our theory, is presented below in logically formed sequence. (a) The stripe alignment problem is solved by construction, thus explaining parallel to the stripe alignment¹¹ of the phonon wave vectors of the phonon anomaly in the untwinned YBCO superconducting crystal. Besides, our theory gives the following important prediction: (b) the anomaly is now caused by the phonon crossing the ubiquitous continuum of 1D charge excitations centered at the intrastripe $2k_F$ (Fig. 1). At the phonon frequency ω , this continuum has a momentum width $\Delta q \approx k_F \omega / v_c$, where v_c is the electronic charge velocity, and this causes a “double-dip,” structure in the phonon spectral function (Fig. 2), as in the transversal stripe mode scenario⁹ (inset of Fig. 2). However, the big

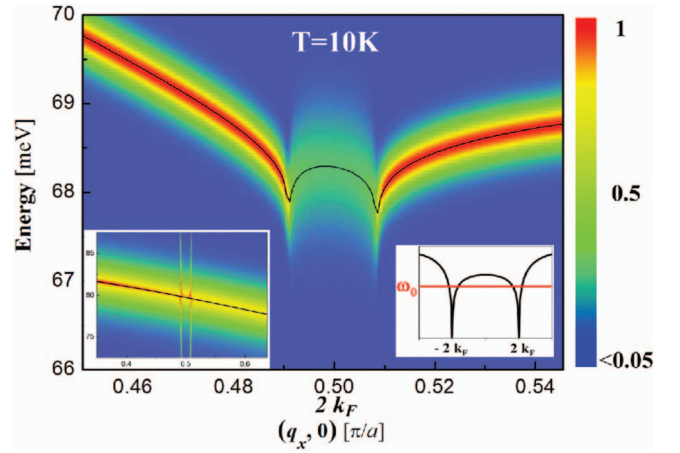


FIG. 2. (Color) False color plot of the LO-phonon spectral function vs momentum in the stripe direction and energy at low temperature (10 K) for 1D $\epsilon_F \sim 0.1$ eV and the same parameters as in Fig. 1. Phonons couple merely to the 1D Fermi-gas-like charge excitations of the metallic electron system confined in the stripes. Strong phonon damping in a momentum region “inside” the anomaly is caused by the decay in the continuum of quasi-1D electron-hole excitations. Left inset: different behavior of the “standard” mode coupling of the phonon with a propagating stripe collective mode (e.g., Ref. 9). Right inset: the renormalized phonon dispersions determined by the crossing of the phonon frequency ω_0 and the real part of the 1D polarization propagator of Fig. 1 (see text).

difference with the prediction⁹ is that in the “smectic scenario,” the phonon is completely (Landau) damped in the momentum region in between the dips; high resolution neutron scattering measurements should be able to resolve this. (c) Another prediction is that the characteristic momentum where the anomaly occurs is now determined by the intrastripe electron density and not by the interstripe distance; hence, the position of the anomaly should have a doping dependence that is radically different from what is expected for transversal modes (Fig. 3). (d) We find a natural explanation for the correlation between the amplitude of the softening strength as a function of doping and the Yamada plot.⁵ (e) We explain why the anomalous phonon linewidth $\Delta\omega$ decreases with increasing temperature (Fig. 4). (f) We show that the form factors of the electron-phonon interaction²¹ localize the phonon anomaly in 2D momentum space also in the direction perpendicular to the stripes (Fig. 4), thus explaining the corresponding experiment.⁴ (g) Counterintuitively, we predict that the transverse width should contract when temperature is raised.

II. ELASTIC MODEL OF THE CuO LAYER IN THE STRIPE PHASE

We embed the array of parallel metallic stripes in the 2D phonon universe by considering a simplified propagator: it describes noninteracting electrons in Bloch states on a periodic array of parallel lines in two dimensions, moving freely

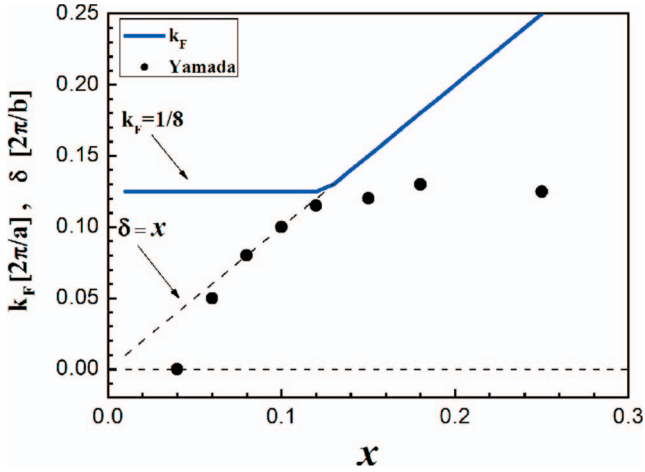


FIG. 3. (Color) The qualitatively different doping dependences expected for the characteristic wave vector of the anomaly when transversal stripe model (1) or the intrastripe quasi-1D electron excitations (2) are responsible. In case (1), the anomaly should follow the stripe-ordering incommensurate wave vector δ dependence on doping x : the famous Yamada plot (Ref. 6) (black dots). Blue line is for the softened phonon wave vector $q=2k_F$ and black dots for the softening strength in case (2).

along these lines, but with vanishing interline overlap of the “Wannier” functions,

$$G(\vec{r}, \vec{r}'; i\omega) = \frac{1}{N_k} \sum_{\vec{k}} \sum_{l, l'=0}^{N-1} \frac{e^{i\vec{k}(\vec{r}-\vec{r}') + iQ(l y - l' y')}}{i\omega - \epsilon(\vec{k})}, \quad (1)$$

where \vec{r}, \vec{r}' span the 1D Cu-centered stripes (lines) in real space and ω is the Matsubara frequency. We consider an orthorhombic Cu-O plane, with a (b) being the unit cell spacing along the x (y) axis. The stripe metallic direction is along the x axis, and the stripe Umklapp momentum $Q = 2\pi/bN$ is along the y axis, where N ($=4$ at higher doping) is the number of unit cells in one interstripe (charge-density) period. The momentum \vec{k} spans N_k sites in the reduced orthorhombic Brillouin zone $0 < k_y < 2\pi/bN$ and $0 < k_x < 2\pi/a$. The electron dispersion $\epsilon(\vec{k}) \approx \epsilon(k_x)$, ignoring interstripe t_{\perp} (see above).

A hole on site \vec{r} inside the stripe communicates with neighboring oxygen bond-stretching displacements $u_{\pm i}^{\vec{r}} \equiv u_i(\vec{r} \pm \vec{i}/2)$, where $\vec{i} = \vec{a}, \vec{b}$, and we take the effective coupling between those and the Zhang-Rice singlets as introduced by Khaliullin and Horsch,²¹

$$H_{e-ph} = g_0 \sum_{\vec{r}} (u_x^{\vec{r}} - u_{-x}^{\vec{r}} + u_y^{\vec{r}} - u_{-y}^{\vec{r}}) c_{\vec{r}}^{\dagger} c_{\vec{r}}, \quad (2)$$

with $g_0 \approx 2$ eV/Å, using the standard estimates for the charge transfer energy and hoppings.²² This is actually our main step: from this Hamiltonian and the 2D “striped”

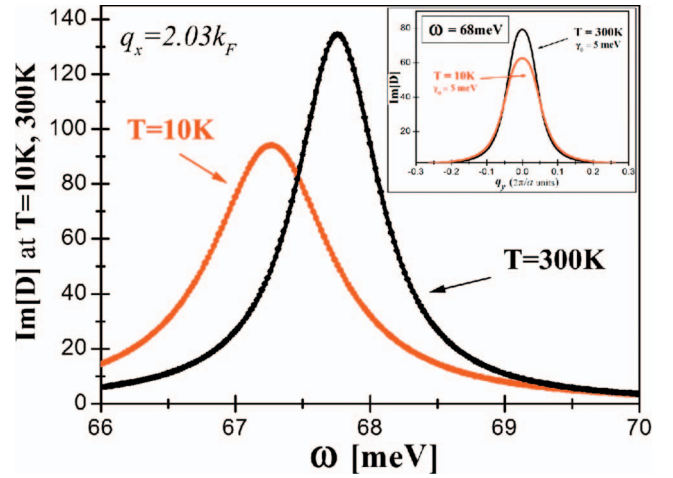


FIG. 4. (Color) Calculated phonon spectral function $\text{Im} D(q_x, q_y=0; \omega)$ dependence on frequency ω , using the same parameters as in Fig. 2, at different temperatures. A temperature narrowing is manifest [in accord with experiment (Ref. 4)], accompanied by a phonon hardening at the dips seen in Fig. 2. Inset: calculated $\text{Im} D(q_x, q_y; \omega)$ momentum dependence in the transversal q_y direction perpendicular to the stripes at fixed $q_x=2k_F$ and $\omega = 68$ meV. Counterintuitively, the anomaly even localizes further when temperature is raised.

electron propagator [Eq. (1)], it is straightforward to calculate the self-energy part of the dynamical matrix associated with the Cu-O plane,

$$\Lambda_{x,y}^{E\alpha,\beta}(\vec{q}, \omega) = \frac{\omega_0}{N_k} \Pi(q_x, \omega) \begin{pmatrix} s_{q_x}^2 & s_{q_x} s_{q_y} \\ s_{q_x} s_{q_y} & s_{q_y}^2 \end{pmatrix}, \quad (3)$$

where ω_0 is bare phonon frequency, $s_{q_x} = \sin q_x a/2$, $s_{q_y} = \sin q_y b/2$, and $\alpha, \beta = 1, 2, 3$ enumerate ions in the in-plane Cu-O unit cell; this particular form of the electron-phonon form factors follows immediately from the tight binding Hamiltonian [Eq. (2)], implying actually a substantial dependence on the momentum q_y perpendicular to the stripes. Here, $\Pi(q_x, \omega)$ corresponds with the polarization propagator of the (in principle, interacting) on-stripe Luttinger liquid, depending on the momentum component q_x along the stripes, while its fermion lines are given by the propagator [Eq. (1)]. The prefactor $1/N_k$ arises because in the $\langle G \times G \sim \Pi \rangle$ product, only terms diagonal in stripe index are retained in the approximation of “independent stripe Luttinger liquids:” there are N_k such terms, while $G \times G \propto 1/N_k^2$ according to Eq. (1).

This self-energy has to be added to the bare (undoped) ab -plane ionic 6×6 dynamic matrix $\Lambda_{ij}^{\alpha,\beta}(\vec{q}, \omega)$ of the orthorhombic planes, constructed to be in close agreement with the experimental data³ for the in-plane bond-stretching LO-phonon modes in the undoped cuprates,

$$\Lambda_{i,j}^{I\alpha,\beta}(\vec{q}, \omega) \propto \begin{pmatrix} \gamma^2(F+G) & 0 & -\gamma F \cos\left(\frac{q_x}{2}\right) & 0 & -\gamma G \cos\left(\frac{q_y}{2}\right) & 0 \\ 0 & \gamma^2(F'+G') & 0 & -\gamma F' \cos\left(\frac{q_x}{2}\right) & 0 & -\gamma G' \cos\left(\frac{q_y}{2}\right) \\ -\gamma F \cos\left(\frac{q_x}{2}\right) & 0 & F & 0 & 0 & 0 \\ 0 & -\gamma F' \cos\left(\frac{q_x}{2}\right) & 0 & F' & 0 & 0 \\ -\gamma G \cos\left(\frac{q_y}{2}\right) & 0 & 0 & 0 & G & 0 \\ 0 & -\gamma G' \cos\left(\frac{q_y}{2}\right) & 0 & 0 & 0 & G' \end{pmatrix}, \quad (4)$$

where $\gamma \equiv \sqrt{\frac{m_O}{m_{Cu}}}$, with m_O and m_{Cu} being, respectively, the oxygen and copper ionic masses, and $q_{x,y}$ is a shorthand for $q_x a$, $q_y b$, respectively. We use $F=0.44$, $F'=0.18$, $G=0.17$, and $G'=0.40$ in units of $\epsilon_F \approx \tilde{t}_{pd}/2 \sim 100$ meV. Here, F is Cu-O coupling constant along the bond a parallel to the x axis, and is slightly bigger than G' , which is Cu-O coupling along the bond b parallel to the y axis. The number of different constants (four) reflects assumed orthorhombic symmetry of the unit cell in the Cu-O plane. This matrix allows for two midbond oxygen atoms surrounding the Cu atom in the in-plane orthorhombic unit cell. We concentrate on the in-plane stretching modes, thus, the apical oxygen degrees of freedom being neglected.

The phonon spectra $\omega_\sigma(\vec{q})$ associated with polarizations $\vec{e}_{\vec{q},\sigma}^\alpha$ are obtained by the diagonalization of the total dynamic matrix.²³ This is done by solving the following dynamic matrix equation:²³

$$\sum_{\beta,j} \{\Lambda_{i,j}^{I\alpha,\beta}(\vec{q}, \omega) + \Lambda_{i,j}^{E\alpha,\beta}(\vec{q}, \omega)\} e_{j,\vec{q},\sigma}^\beta = \omega_\sigma^2(\vec{q}) e_{i,\vec{q},\sigma}^\alpha. \quad (5)$$

From these solutions, the phonon spectral functions given by the imaginary part of the phonon propagator $D(\vec{q}, \omega)$ are obtained. Notice that the Λ^E are, in general, complex quantities, with the effect that $\omega_\sigma(\vec{q})$ acquires an imaginary part representing the phonon damping.

III. "FINGERPRINTS" OF ONE-DIMENSIONAL STRIPE POLARIZATION IN THE BOND-STRETCHING PHONON ANOMALY

We use for $\Pi(q_x, \omega)$ the well-known 1D Lindhardt function,²⁴

$$\text{Re } \Pi(q, \omega) = -\frac{\omega_0 \xi}{4\pi q \tau} \int_0^\infty \ln \left| \frac{\Delta_+}{\Delta_-} \right| ch^{-2} \left(\frac{p^2 - 1}{2\tau} \right) p dp, \quad (6)$$

$$\text{Im } \Pi(q, \omega) = \frac{\omega_0 \xi}{8} \left[th \frac{\omega + 2(q-2)}{4\tau} + th \frac{\omega - 2(q-2)}{4\tau} \right], \quad (7)$$

here, $\Delta_\pm = (2p \pm q)^2 q^2 - \omega^2$, all momenta and energies are measured in units of the Fermi-gas parameters k_F and $\epsilon_F \equiv k_F^2/2m \sim 0.1$ eV, and $\tau = k_B T / \epsilon_F$ is a dimensionless temperature. The dimensionless electron-phonon coupling constant $\xi = g_0^2 / K \epsilon_F \sim 1$ is representative for cuprates with $K \approx 25$ eV/Å², the lattice force constant.²¹

A. Doping dependences of the phonon anomaly

The effect of this 1D polarizability on the phonons follows from the behavior of $\Pi(q_x, \omega)$ at the phonon frequency $\omega = \omega_0$ as a function of q_x (Fig. 1). The continuum of charge excitations in a 1D Fermi-gas is the well-known fan in the momentum-frequency plane, centered at $2k_F$ at $\omega=0$ and bounded by $2k_F \pm \omega/v_F$ at finite frequency. For noninteracting electrons, the spectral function ($\text{Im } \Pi$) is just the box of Fig. 1, while in the presence of interactions, the spectral weight will pile up at the edges. Since Π is proportional to the phonon self-energy, the phonon spectral function (Fig. 2) indicates that the phonon dispersion is pushed downward when it approaches the edges of the quasi-1D electron-hole continuum from either sides to broaden strongly when it enters the continuum. This is markedly different from the result based on a mode coupling between the phonon and a propagating mode as, for instance, discussed by Kaneshita *et al.*⁹ and as shown in the inset of Fig. 2; in this case, there is no phonon damping, and the intensity is just distributed over the propagating modes subjected to an avoided level crossing. The bottom line is that the gross effect of the two scenarios is quite similar, and to find out the difference, higher resolution measurements are required.

A distinction between the effects of the transversal stripe modes and the internal 1D-like fermionic excitations on the phonon anomaly should be as well revealed by the different

doping dependences of the locus of the phonon anomaly in momentum space. The transversal fluctuations emerge at the stripe-ordering wave vectors and these should follow the famous Yamada plot,⁶ correlating the stripe-ordering wave vectors δ with doping x (Fig. 3), such that at low dopings, the anomaly should live at a wave vector $q_a \sim 1/x$. On the other hand, dealing with the quasi-1D modes, the locus of the anomaly is determined by the on-stripe hole density, and according to the Yamada plot, this stays constant (“half-filled”) at $q_a = 2k_F = \pi/2a$ up to $x_c = 1/8$, while at higher dopings $x > x_c$, it should follow $q_a = 2k_F \propto x$ because the on-stripe hole density is increasing (the blue line in Fig. 3). Experimentally, the locus of the anomaly in k space is conspicuously doping independent,³ actually arguing strongly against the transversal mode. It would be interesting to find out if the “center of mass” of the anomaly does shift at higher dopings. Remarkably, the prefactor $1/N_k$ in the phonon self-energy [Eq. (3)] and, hence, the softening amplitude $\Delta\omega \propto \Pi/N_k$ depends on doping x roughly in the same way as given by the Yamada plot⁶ (black dots in Fig. 3). This should be true for both the amplitude of the sharp feature around $q_a \sim 2k_F = \pi/2a$ (the double dip in Fig. 2) as well as for the amplitude of the “smooth” softening across the half Brillouin zone caused by the momentum-dependent form factors $s_{q_{xy}} = \sin q_x a/2$ and $\sin q_y b/2$ in 2×2 matrix multiplied by Π/N_k in Eq. (3). This latter fact may explain naturally why the amplitude A in the phenomenological function of $0.5A \cos q_x a + B$ follows Yamada plot as a function of hole doping x (see Fig. 4 of Ref. 5), as long as this function is used⁵ to fit smooth part of the measured bond-stretching phonon softening in $\text{La}_{2-x}\text{Sr}_x\text{CuO}_4$.

B. Temperature and wave vector dependences of the phonon anomaly

Our theory yields a rationale for the observed gross temperature dependences of the anomaly.⁴ The rather counterintuitive narrowing of the frequency width with increasing temperature follows naturally from the temperature dependence of the 1D polarization propagator: $\text{Im } \Pi \propto \omega/T$ (Fig. 1). The effect of this change on the phonon-spectral function is shown in Fig. 4: a substantial narrowing occurs at higher temperature. Moreover, right at the “dips,” a substantial phonon hardening occurs since the phonon positions at these

momenta are most sensitive to the details of the real part of the self-energy.

The phonon anomaly behavior in the “transversal” q_y direction (inset of Fig. 4) follows from our analysis of the expression for the phonon spectral function $\text{Im } D(q_x, q_y; \omega)$, showing a substantial q_y dependence close to the anomaly due to the form factors in Eq. (3),

$$\text{Im } D(q_x, q_y; \omega) \approx \frac{\omega_0 \Delta_{q_x, q_y} \text{Im } \Pi_{q_x}}{4(\tilde{\omega}_{q_x, q_y} - \omega)^2 + \Delta_{q_x, q_y}^2 \text{Im}^2 \Pi_{q_x}}, \quad (8)$$

where $\Delta_{q_x, q_y} \equiv s_{q_x}^2 + s_{q_y}^2$ and $\tilde{\omega}_{q_x, q_y} \approx \omega_0 + 0.5 \Delta_{q_x, q_y} \text{Re } \Pi_{q_x}$ is the renormalized optical phonon mode frequency. The width of the Lorentzian with respect to q_y at $\omega = \tilde{\omega}_{q_x, q_y=0}$ is $\delta q_y \approx 2/a \sqrt{|\text{Im } \Pi / \text{Re } \Pi|} \sim 0.1 \times 2\pi/a$, assuming a flat bare mode dispersion. Given the ratio under the square root, the width δq_y decreases when the temperature is raised.

IV. CONCLUSIONS

In summary, we have analyzed a minimal, (over) simplified model dealing with the Luttinger-liquid-like excitations coming from the electrons confined in stripes interacting with optical lattice phonons. Our main finding is that the gross features of the phonon anomaly as measured experimentally are consistent with the workings of a quasi-1D array of metallic intrastripe Luttinger liquids. Their “fingerprints” described above include binding of the anomalous phonon momentum to 1D intrastripe $2k_F$ wave vector and hence to its doping dependence, a Yamada plot behavior of the softening strength, a decrease with increasing temperature of the phonon linewidth and of the spread of the anomaly in the transverse momentum, and a double-dip structure of the bond-stretching phonon anomaly that should be observable at high enough resolution.

ACKNOWLEDGMENTS

The authors appreciate stimulating discussions with D. Reznik. We acknowledge financial support by the Netherlands Foundation for Fundamental Research of Matter (FOM) and the Dutch organization for scientific research (NWO). S.I.M. acknowledges support by a Royal Society (UK) grant for international incoming short visits and RFBR grant (07-02-12058) by Russian Academy of Sciences.

*sergeimoscow@online.ru

¹R. J. McQueeney, Y. Petrov, T. Egami, M. Yethiraj, G. Shirane, and Y. Endoh, Phys. Rev. Lett. **82**, 628 (1999).

²L. Pintschovius, W. Reichardt, M. Klaser, T. Wolf, and H. v. Lohneysen, Phys. Rev. Lett. **89**, 037001 (2002).

³L. Pintschovius, D. Reznik, W. Reichardt, Y. Endoh, H. Hiraka, J. M. Tranquada, H. Uchiyama, T. Masui, and S. Tajima, Phys. Rev. B **69**, 214506 (2004); L. Pintschovius, Phys. Status Solidi B **242**, 30 (2005).

⁴D. Reznik, L. Pintschovius, M. Ito, S. Iikubo, M. Sato, H. Goka,

M. Fujita, K. Yamada, G. D. Gu, and J. M. Tranquada, Nature (London) **440**, 1170 (2006); D. Reznik, L. Pintschovius, M. Fujita, K. Yamada, G. D. Gu, and J. M. Tranquada, J. Low Temp. Phys. **147**, 353 (2007).

⁵T. Fukuda, J. Mizuki, K. Ikeuchi, K. Yamada, A. Q. R. Baron, and S. Tsutsui, Phys. Rev. B **71**, 060501(R) (2005).

⁶K. Yamada, C. H. Lee, K. Kurahashi, J. Wada, S. Wakimoto, S. Ueki, H. Kimura, Y. Endoh, S. Hosoya, G. Shirane, R. J. Birgeneau, M. Greven, M. A. Kastner, and Y. J. Kim, Phys. Rev. B **57**, 6165 (1998).

- ⁷J. Zaanen, *Nature (London)* **440**, 1118 (2006).
- ⁸P. Abbamonte, A. Rusydi, S. Smadici, G. D. Gu, G. A. Sawatzky, and D. L. Feng, *Nat. Phys.* **1**, 155 (2005).
- ⁹E. Kaneshita, M. Ichioka, and K. Machida, *Phys. Rev. Lett.* **88**, 115501 (2002).
- ¹⁰H. Eskes, O. Y. Osman, R. Grimberg, W. van Saarloos, and J. Zaanen, *Phys. Rev. B* **58**, 6963 (1998).
- ¹¹H. A. Mook, P. Dai, F. Dogan, and R. D. Hunt, *Nature (London)* **404**, 729 (2000).
- ¹²J. Zaanen and O. Gunnarsson, *Phys. Rev. B* **40**, 7391 (1989); J. Zaanen and A. M. Oles, *Ann. Phys.* **5**, 224 (1996).
- ¹³S. A. Kivelson, E. Fradkin, and V. J. Emery, *Nature (London)* **393**, 550 (1998); S. A. Kivelson, I. P. Bindloss, E. Fradkin, V. Oganesyan, J. M. Tranquada, A. Kapitulnik, and C. Howald, *Rev. Mod. Phys.* **75**, 1201 (2003); E. Arrigoni, E. Fradkin, and S. A. Kivelson, *Phys. Rev. B* **69**, 214519 (2004).
- ¹⁴S. I. Mukhin, arXiv:cond-mat/0507294 (unpublished).
- ¹⁵V. I. Anisimov, M. A. Korotin, A. S. Mylnikova, A. V. Kozhevnikov, D. M. Korotin, and J. Lorenzana, *Phys. Rev. B* **70**, 172501 (2004).
- ¹⁶X. J. Zhou, P. Bogdanov, S. A. Kellar, T. Noda, H. Eisaki, S. Uchida, Z. Hussain, and Z.-X. Shen, *Science* **286**, 268 (1999).
- ¹⁷X. J. Zhou, T. Yoshida, S. A. Kellar, P. V. Bogdanov, E. D. Lu, A. Lanzara, M. Nakamura, T. Noda, T. Kakeshita, H. Eisaki, S. Uchida, A. Fujimori, Z. Hussain, and Z.-X. Shen, *Phys. Rev. Lett.* **86**, 5578 (2001).
- ¹⁸T. Yoshida, X. J. Zhou, K. Tanaka, W. L. Yang, Z. Hussain, Z.-X. Shen, A. Fujimori, S. Sahrakorpi, M. Lindroos, R. S. Markiewicz, A. Bansil, S. Komiya, Y. Ando, H. Eisaki, T. Kakeshita, and S. Uchida, *Phys. Rev. B* **74**, 224510 (2006).
- ¹⁹K. Gofron, J. C. Campuzano, A. A. Abrikosov, M. Lindroos, A. Bansil, H. Ding, D. Koelling, and B. Dabrowski, *Phys. Rev. Lett.* **73**, 3302 (1994).
- ²⁰Y. Kohsaka, C. Taylor, K. Fujita, A. Schmidt, C. Lupien, T. Hanaguri, M. Azuma, M. Takano, H. Eisaki, H. Takagi, S. Uchida, and J. C. Davis, *Science* **315**, 1380 (2007).
- ²¹G. Khaliullin and P. Horsch, *Physica C* **162-164**, 462 (1989); P. Horsch and G. Khaliullin, *Physica B* **359-361**, 620 (2005).
- ²²F. Barriquand and G. A. Sawatzky, *Phys. Rev. B* **50**, 16649 (1994).
- ²³C. Falter, *Phys. Rep.* **164**, 1 (1988).
- ²⁴B. Horowitz, H. Gutfreund, and M. Weger, *Phys. Rev. B* **12**, 3174 (1975).